

A Comparison Study of Removing Rhodamine B from Wastewater by Nitric Acid Functionalized Rice Husk, Coconut Husk and Synthetic Porous Carbon



Charitha Thambiliyagodage, Sulakshini Ranchagoda,
and Shanitha Mirihana

Abstract The present comparison study describes the effectiveness of different carbon based adsorbents for the successful removal of Rhodamine B (RhB) from wastewater. Selected adsorbents are rice husk (RH) and coconut husk (CH) as the agricultural waste products and porous carbon synthesized by resorcinol formaldehyde polymerization via sol gel method (SC). Such porous materials were functionalized using nitric acid. Morphology of the materials were examined by the Scanning electron microscope (SEM) and the surface functionalities were determined by FT-IR spectroscopy. Adsorption of all functionalized and raw porous materials was determined by varying parameters such as pH of the medium, adsorbent dosage, dye concentration and contact time. Generally, all the selected adsorbents were capable of removing RhB and functionalized adsorbents were much effective than the untreated adsorbents. Among all the adsorbents selected for the comparison, functionalized rice husk (FRH) showed highest activity compared to other adsorbents as it consists of both carbon and silica, while others have only carbon. Interestingly adsorbents prepared by natural waste materials were more effective than the synthetic carbon suggesting that these tested materials could be used in novel water purification systems to decontaminate waste and drinking water.

Keywords Rice husk · Coconut husk · Resorcinol–formaldehyde · Nitric acid · Rhodamine B · Wastewater

Charitha Thambiliyagodage and Sulakshini Ranchagoda—are contributed equally.

C. Thambiliyagodage (✉) · S. Mirihana
Faculty of Humanities and Sciences, Sri Lanka Institute of Information Technology, Malabe, Sri Lanka
e-mail: charitha.t@slit.lk

S. Ranchagoda
Institute of Chemistry Ceylon, Adamantane House, 341/22, Kotte Road, Rajagiriya, Sri Lanka

1 Introduction

Synthetic dyes are extensively used in industrial applications including textile [24], paper [22], food [11] and paint [1] industries. Such dyes are classified into different groups depending on their chemical structure as azo, anthraquinone, sulphur, phthalocyanine, and triarylmethane [32]. Azo dyes consisting of two nitrogen groups are quantitatively the most important group and being the most problematic pollutant of wastewater originated by dye discharging sources. The release of dye contaminated wastewater to natural habitats is hazardous not only to the aquatic life disturbing the natural equilibrium but also to the human beings causing allergies, dermatitis, skin irritations [5, 6, 20]. Hence, the removal of dyes from effluents before they are released to the natural water reservoirs is of great importance. Many methods have been reported to remove such dyes from wastewater by adsorption [18, 26, 44], photocatalytic degradation [7, 14, 17], electrochemical methods [42] and coagulation-flocculation [25], of which adsorption has been found to be the most promising method. Decoloration of wastewater by adsorption of dyes by Activated carbon has been found to be very efficient due to its high surface area, porous structure, high degree of surface functionality and high adsorption capacity [4, 13, 28]. However, commercially available activated carbon is very expensive and has high regeneration cost. Hence, researchers are interested in finding alternative materials which are efficient, inexpensive and easily available [4]. Different adsorbents such as alumina [3], silica [2, 21], zeolites [43], which have been reported as other alternatives and naturally available waste materials like orange peel [37], rice husk [29], saw dust [12], coir pith [31], straw [23] have been used to produce functionalized activated carbon as potential candidates to remove dyes from wastewater. It is vital to use low cost waste materials as adsorbents to remove dyes from contaminated water basically due to two reasons. Disposal of such waste materials generated by agriculture, industry or any other means is problematic and regeneration of spent materials as adsorbents is unnecessary due to the low cost and abundance. Hence, it is important to develop an inexpensive, abundant and efficient adsorbent from waste materials for the removal of industrial pollutants. From our previous study we have shown that non-functionalized rice husk is capable of removing methylene blue, methyl orange and metal ions like Pb^{2+} , Cu^{2+} , Cd^{2+} and Ni^{2+} [41]. Continuing such interest, a comparative study was carried out using nitric acid treated porous carbon originated by paddy husk and coconut husk as the agricultural waste materials and carbon synthesized by resorcinol–formaldehyde polymerization to remove RhB from artificial wastewater.

2 Materials and Methods

2.1 Materials

Rhodamine B was supplied by Prym Intimates Lanka (Pvt.) Ltd., Lot 16–17. Biyagama EPZ, Walgama, Malwana, Sri Lanka. Rice husk was collected from Nawagamuwa area and coconut husk was collected from Kuliyaipitiya area, Sri Lanka country. Polyethylene glycol 20,000 (PEG), and Cetyl triammonium bromide (CTAB), HCl, HNO₃, NaOH, Formalin, Ethylenediamine were procured from Sisco Research Laboratories (Pvt.) Ltd, India.

2.2 Instrumentation

Fluorescence emissions were recorded on a Fluorescence spectrophotometer (Model: HITACHI F-2700) and the FT-IR spectra were collected by a ABB MB3000, Canada FTIR using ATR device. Scanning electron microscopic images were taken by Hitachi SU6600 Analytical Variable Pressure FE-SEM.

2.3 Methods

2.3.1 Preparation of Carbonaceous Materials

RH from paddy that are harvested in Sri Lanka were employed as the raw material. The soil and dust in the rice husks were washed with distilled water and ethanol and dried at 80 °C. Then the purified RH was separately treated with 2 mol dm⁻³ HCl acid at 60 °C for 2 h with regular stirring. Acid leached RH was rinsed with distilled water until the pH of the filtrate reaches ~ 6 and was dried at 80 °C. Then RH was placed in a muffle furnace and heated at 400 °C for 2 h to obtain acid leached RHA. CH obtained from Sri Lanka was used to produce the coconut based porous carbon adsorbent. CH was washed with distilled water and ethanol many times to remove all the dust and solid particles followed by drying at 80 °C and a portion of it was carbonized as mentioned above.

Hierarchically porous monolithic carbon was synthesized by dissolving resorcinol (3 g) in a solvent mixture of ethanol (11.5 mL) and distilled water (9 mL) followed by addition of 1.5 g of PEG with constant stirring at room temperature. Mixture was stirred until all PEG dissolves and 1.5 g of CTAB was added to the mixture. Once all the CTAB dissolves in the solvent mixture 0.1 g of ethylenediamine was added and the mixture was stirred for 30 min. Formalin containing formaldehyde (4.5 g, 35 wt%) was quickly added to the mixture. The reaction mixture was stirred further for 10 min and the resulting homogeneous emulsion in closed vessels were transferred

to an oven and were heated at 80 °C for 4 h. Resulting gels were dried at 50 °C for 2 days and were carbonized at 400 °C for 2 h.

All the prepared carbon based porous adsorbents were functionalized with 6 M HNO₃ acid at 60 °C for 6 h with regular stirring. After the treatment, adsorbents were rinsed with distilled water until the pH of the washings reached ~ 6 and was dried at 80 °C. The dried samples was sifted through sieves of 0.5 mm pore size and stored in a desiccator until further use. Hereafter, all functionalized RH, CH and SC adsorbents will be labeled in the text as FRH, FCH and FSC, respectively.

2.3.2 Preparation of RhB Solutions

A stock solution of 100 mg/L was prepared by dissolving accurately weighed sample of dye in a 250 mL of distilled water. The desired experimental concentrations of dye solutions were prepared by the appropriate dilutions of the stock solution in distilled water. The pH of each solution was adjusted by adding diluted HCl or NaOH solution and measured with a benchtop meter.

2.3.3 Batch Study

The effect of experimental parameters of pH (2–10, step size: 2), initial dye concentration (5–20 mg/L, step size: 5 mg/L), and adsorbent dosage (5–30 mg, step size: 5 mg) were studied in the batch mode for a total of 60 min. RH was incubated for 2 h and as the equilibrium reached in 60 min, other two adsorbents were incubated only for one hour to be consistent with RH to compare their results. pH of the medium was not changed and kept that of distilled water for all the experiments except at the pH optimization. In each adsorption experiment, 25 mL sample of RB solution with known concentration was transferred to a 50 mL centrifuge tube, and known weight of the adsorbent was added into the tube and they were shaken for 1 h at 200 rpm in the orbital shaker. Except for the experiments of which effect of RB concentration was supposed to determine, concentration was kept constant at 5 mg/L. Similarly, the weight of porous carbon material was kept constant at 25 mg in all experiments, where it was only varied at mass optimization experiment. The concentration of RB solution was determined by using a Fluorescence spectrophotometer of which the wavelength range was adjusted to 564–574 nm. The adsorption capacity was calculated by using the following equation:

$$qt = V \frac{C_o - C_t}{m}$$

where C_o and C_t were the initial concentration and the concentration at time t in mg/L respectively, m was the mass of the adsorbent in g, and v was the volume of the solution in L. The removal efficiency was calculated using the following equation:

$$E = \frac{C_o - C_t}{C_o} 100\%$$

2.3.4 Reusability of the Adsorbent

Functionalized adsorbent (30 mg) was dispersed in 25 mL of 5 mg/L RhB solution was shaken for 1 h. The used adsorbent was isolated and was washed with distilled water and ethanol until the washings had no pink colour. Washed adsorbent was used again with the same experimental conditions. After each run the concentration of the remaining RB in the solution was determined.

3 Results and Discussion

3.1 Material Characterization

3.1.1 Material Synthesis

Hierarchically porous carbon was synthesized by a modified procedure [19, 41]. Resorcinol and formaldehyde are the precursors of the polymerization while PEG is the macropore directing agent and CTAB is the mesopore directing agent. Ethylene-diamine provides the required basicity to the reaction medium acting as a catalyst for the polymerization. In addition it act as a crosslinking agent and provides N based functional groups to the carbon structure as well [19].

3.1.2 SEM Analysis

Scanning electron microscopic images of the adsorbents were taken in order to study the morphology. RH has a naturally available irregular shaped macropore structure which lead to macropore channels as shown in the Fig. 1a. CH also show irregular shaped macropores which are much oriented. Further they have formed ordered macropore tubes as shown in the Fig. 1b. SEM images of SC (Fig. 1c) show spherical, eclipse shaped, and irregular shaped macropores with a wide variation in size are scattered in the matrix of carbon without interconnectivity. These macropores also form macropore channels but they are disordered. The solvent to polymer ratio affect the morphology of the macropores, the size of the macropores and the skeleton and the interconnectivity of the macropores. The observed macropore structure of SC resulted due to the small ratio of solvent to polymer used in the synthesis [27]. Macropores are formed during the spinodal decomposition. When resorcinol is mixed with

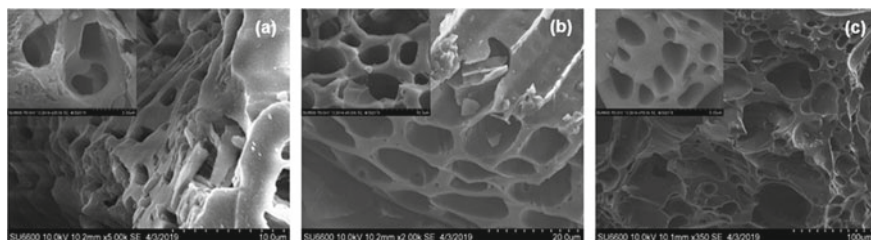


Fig. 1 SEM images of **a** RH, **b** CH, **c** SC

PEG, they form H bonds with each other. During the prepolymerization formaldehyde copolymerized with resorcinol and form oligomers and the solubility of the polymer mixture in the alcoholic solution decreases separating polymer phase from the alcoholic solvent. After prepolymerization, the solution was heated and hence the immiscibility progress with concomitant polymerization. This is known as polymerization induced phase separation. The phase separation could develop from either spinodal decomposition or bimodal decomposition. Bimodal decomposition causes the appearance of isolated spherical domains as resulted in this synthesis as shown in the Fig. 1c. Bicontinuous microstructures are developed by spinodal decomposition and such system has not developed in this work as shown by the SEM images [27]. Mesopores should be originated from the soft template method where CTAB form a micelle structure and resorcinol interacts with CTAB via electrostatic interactions [8]. During the carbonization these CTAB molecules are burnt off resulting mesopores. Micropores are generated during the carbonization process where small molecules are removed from the carbon matrix and resulting small voids create micropores if the diameter is less than 2 nm and mesopores if the diameter is greater than 2 nm.

3.1.3 FT-IR Analysis

Adsorption capacity of an adsorbent depends on the porosity of the adsorbent and the density of the surface functional groups present. Generally, carbon based adsorbents have functional groups based on heteroatoms such as carbon, oxygen, nitrogen and sulfur. FT-IR analysis was performed for all the samples and the acquired FT-IR spectra are given in the Fig. 2. FT-IR spectra of RH and FRH are given in Fig. 2a. The band at 1095 cm^{-1} can be assigned to the Si–O–Si stretching, the shoulder band around 800 cm^{-1} to Si–O bending and Si–OH stretching collectively and the band at 465 cm^{-1} to Si–O out of plane deformation [36]. FT-IR spectra of CH and FCH, and SC and FSC are given in Fig. 2b, c respectively. The broad peak appeared $3300\text{--}3500\text{ cm}^{-1}$ which is more apparent in the functionalized adsorbents can be attributed to the OH stretching [39]. The wide peak at $(1540\text{--}1650\text{ cm}^{-1})$ shows the presence of asymmetric stretch of the COO^- group [38] and the peak at 1046 cm^{-1} shows the presence of C–O–C functional group [30, 39]. The peaks correspond to the above functional groups which are related to the COOH are high in intensity in

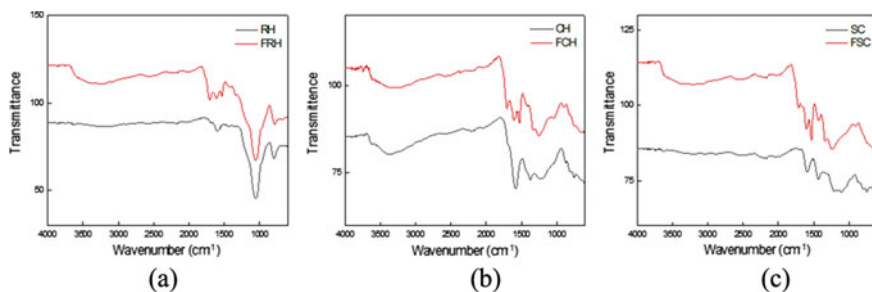


Fig. 2 FT-IR Spectra of **a** RH and FRH, **b** CH and FCH, **c** SC and FSC

the functionalized adsorbents clearly suggest that the surface of the adsorbents have oxidized by concentrated nitric acid treatment agreeing with the mechanism proposed by Zhang et al. that HNO_3 acid oxidize the surface of the carbon introducing COOH groups [46].

3.1.4 Effect of pH

pH is one of the main parameter that controls the adsorption of adsorbates to adsorbents. The pH of the solution was adjusted by the addition of HCl and NaOH. Variation of adsorption capacity with pH is shown in Fig. 3. The structure of RhB changes with changes in the pH. At low pH values where the medium is highly acidic RhB exists in the cationic and monomeric form [10, 34]. Thus, RhB molecule can penetrate the porous structure of the adsorbents. At pH values higher than 4 the zwitterion form exists and upon alkalization the zwitterion form predominates and it may increase the aggregation of the RhB molecules. RhB molecules aggregated due to the attractive electrostatic interactions between the carboxyl group and the xantheno groups of the monomer. Hence, aggregated RhB molecules or dimers of RhB will not easily penetrate through the porous structure of the adsorbents. At high pH, abundantly available OH^- creates a competition between the $-\text{N}^+$ and COO^-

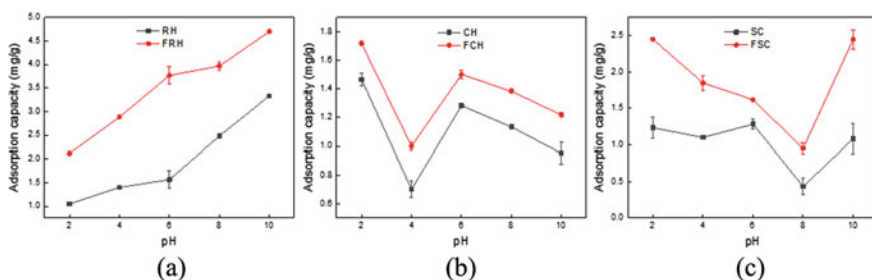


Fig. 3 Effect of pH on adsorption of RhB on **a** RH and FRH, **b** CH and FCH, **c** SC and FSC

and decreases the aggregation of RhB increasing the adsorption RhB to the adsorbate surface [10, 34].

Nitric acid was used to functionalize the adsorbate surface. Highly concentrated nitric acid oxidize the surface of the adsorbents FRH, FCH, and FSC introducing $-\text{COOH}$ and lactone groups to the adsorbent surface. In addition carbon surfaces consist of Nitrogen based functional groups especially in synthetic carbon where nitrogen was introduced by ethylenediamine. These functional groups get protonated at lower pH values and get deprotonated at high pH values. However, the net charge of the adsorbent surface and the attraction or repulsion interactions between the adsorbent and RB cannot explain the adsorption behavior of RB with varying pH values. Adsorption capacity of RH and FRH increases from 1.05 mg/g and 2.12 mg/g respectively, at pH 2 to 3.33 mg/g and 4.70 mg/g respectively, at pH 10. RH mainly consists of carbon and silica where silica provides additional negative charge to the adsorbent compare with CH and SC. At acidic pH of 2, and 4 and even at pH 6 where the cationic form of RhB is predominant, RhB molecules have interacted with the RH and FRH surface though the charge of the adsorbent surface is not a principal factor that determines the adsorbent adsorbate interactions. Moreover, as carbon and silica both components of RH contain pores of different sizes, different size of RhB as monomers and aggregates could still get into the porous structure. Since silica tend to dissolve at higher pH values, diameter of the pores of silica tend to increase with the dissolution of the pore walls facilitating larger molecules to migrate through the pores. Hence the adsorption capacity of both RH and FRH increases with increasing pH. Adsorption capacity of FRH is higher than that of RH due to the new functional groups introduced to the adsorbent surface such COOH , lactone as indicated by the FT-IR spectra as given in the Fig. 2a.

Adsorption capacity of SC and FSC decreases generally with increasing pH up to 8 and increases to a maximum of 1.23 mg/g and 2.45 mg/g respectively, at pH 10. Adsorption capacity of SC and FSC at pH 2 shows highest adsorption capacity as the cationic RhB molecules can easily pass through the porous system and get adsorb to the carbon surface. As the pH increases to pH 8 the monomeric cationic RhB gradually converts to its zwitterion form and results in aggregated (dimer like) RhB molecules. The macropores present in SC are large in size and have only few in a given area compared with RH and CH where the amount of macropores is high in a given area. Presence of mesopores and micropores does not affect the adsorption of aggregated RhB molecules as they cannot enter such small pores. Thus, the limiting factor is the amount of macropores and hence, when the pH increases the resulting penetration and adsorption of aggregated RhB molecules is comparatively low. But when the pH increases to 10 due to alkalinity the aggregation of RhB molecules is prevented and adsorption of RhB increases. CH and FCH show a different behaviour where the adsorption capacity decreases from pH 2–4 and then increases at pH 6 and again decreases gradually to pH 10. It is evident that the adsorption capacity of RhB by CH and FCH is high at pH as the cationic monomeric RhB easily adsorb to the adsorbent surface. However, that has drastically reduced at pH 4 and again increases to pH 6 which reduces till pH 10. pK_a of RhB is 3.7 and transformation of the cationic form to zwitterionic form starts at pH greater than the pK_a [30]. As the pH

increases from 2 to 4 the availability of OH^- groups increase and may have initiated the aggregation of RhB resulting lower adsorption capacity. When the pH increases to $\text{pH} = 6$, medium is almost neutral and dimeric form of RhB molecules may exist in addition to the monomeric RhB resulting high adsorption capacity relative to $\text{pH} 4$. Meanwhile beyond $\text{pH} 6$ adsorption capacity again decreases which could be due to the surface charge of the material. Surface become more negatively charged as the pH increases and the zwitterion form and the lactone form of RhB which predominates at high pH values would have been repelled by the surface of the adsorbent. Further as described above as the RhB aggregates entrance of the molecules to the porous structure become difficult resulting low adsorption capacities at high pH values. Interestingly, the adsorption capacity of CH is higher than FCH only when the pH of the medium is changed indicating the H^+ and OH^- concentrations of the medium and hence the surface charge of the adsorbent have significant influence in adsorption. However, the surface charge of the adsorbent has played a crucial role in adsorbing RhB to CH being different from RH and SC. Moreover, the adsorption capacity of RH species (RH and FRH) is higher than both CH and SC species, which could be attributed to the presence of two different main components, carbon and silica in the same adsorbent while others are single component adsorbents (carbon only). RH has carbon and silica as the components and in both low and high pH silica tend to dissolve [45]. The dissolution of the adsorbent in such conditions is a problem and hence all the rest of studies were performed at neutral pH though the three different adsorbents showed three different optimum pH values of maximum adsorption.

3.1.5 Effect of Adsorbent Dosage

The effect of adsorbent dosage on adsorption have been determined by adding varying weights of adsorbents to a fixed volume and initial concentration of RhB and by shaking for a fixed time. The efficiency of RhB removal by RH and FRH increases with increasing mass of the adsorbent as shown in the Fig. 4a. The removal efficiency

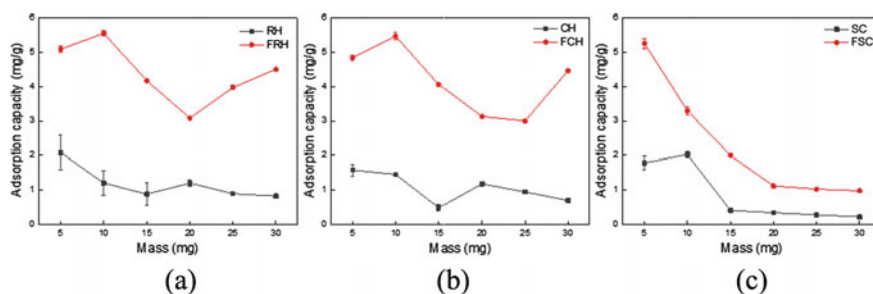


Fig. 4 Effect of adsorbent dosage on adsorption of RhB on **a** RH and FRH, **b** CH and FCH, **c** SC and FSC

is comparatively high in FRH than RH at all the adsorbent dosages. At higher adsorbent weights like 20, 25, 30 mg, efficiency drastically increases in FRH compared to RH of which efficiency is almost the same. This could be attributed to the fact that high concentration of functional groups have been created on the adsorbent surface during functionalization exposing enough adsorption sites to the adsorbates. But in RH only the weight of the mass was increased and the functionalities has not proportionally increased resulting same removal efficiencies. However, the adsorbent capacity of both RH and FRH do not have a particular trend. The increase in adsorption capacity of FRH from 5 to 10 mg resulted due to the strong driving force and high surface area. Adsorption capacity of FRH decreases with increasing adsorbent dosage from 10 to 20 mg because there is a less commensurate increase in adsorption with the rise in the adsorbent dosage. On further increment of adsorbent weight from 20 to 30 mg adsorption capacity increases slowly due to the available high concentration of functional groups introduced and due to the predominant adsorption, and intraparticle diffusion taking place simultaneously [16, 33]. Above described net behavior of removal efficiency and adsorption capacity was also observed with CH and FCH as given in the Fig. 4b. However, in SC and FSC a different behavior was observed as shown in the Fig. 4c. Adsorption capacity of SC increases from 5 to 10 mg but drastically decreases from 10 to 15 mg and then gradually decreases. Rise of adsorption capacity initially of SC could be attributed to the available high surface area and the strong driving force of RhB molecules as described with FRH. Decrease of adsorption capacity of SC afterwards and totally in FSC with increasing weight of the adsorbent could be due to the agglomeration of the adsorbent particles reducing the surface area and covering of the adsorption sites [9]. Efficiency of both FSC and SC initially increases when weight of the adsorbent increase from 5 to 10 mg and then decreases from 10 to 20 mg. Efficiency of SC generally remain constant afterwards while that of FSC increases again. A clear increasing trend of efficiency with increasing weight of both SC and FSC was not observed because the reduction in the concentration of RhB in the solution varies which could be due to the irregularity of the functional groups distribution on the adsorbent surface, adsorbent particles agglomeration, disordered nature of the porous system, challenges in transport of RhB to the adsorbate surface etc.

3.1.6 Effect of Initial Dye Concentration

The effect of variation in the initial dye concentration of RhB (5–20 mg/L) was carried out using 30 mg of the adsorbent for 60 min. The data indicate that the adsorption capacity decreases with increasing concentration of RhB in all adsorbents as given in the Fig. 5. At lower concentrations, the ratios of RhB molecules to the available adsorption sites and the surface area were low, resulting high adsorption capacity [35, 40]. But at higher concentration available adsorption sites become limited reducing the adsorption. Adsorption capacity decreases with increasing RhB concentration because with increasing concentration the amount of RhB adsorbed decreases though the weight of the adsorbent is constant.

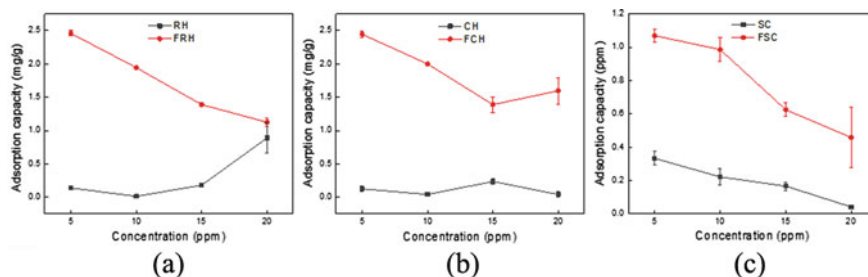


Fig. 5 Effect of initial dye concentration on adsorption of RhB on **a** RH and FRH, **b** CH and FCH, **c** SC and FSC

Adsorption capacity of RH increased at higher concentrations. It is only the carbon component get functionalized with nitric acid treatment and not the silica component of RH normally. So introduced adsorption sites to carbon become the limiting factor in RhB adsorption at increasing concentrations of RhB on FRH only and not in RH. Once the RhB molecules adsorb to the surface of the FRH the surface get crowded from the bulky RhB molecules restricting the penetration of unadsorbed RhB molecules to the deep active sites present in the porous structure. However, in RH as the surface is not functionalized the surface will be much available facilitating the penetration of RhB molecules to the porous structure of both carbon and silica. At increasing RhB concentrations comparatively high amount of RhB get adsorbed to the adsorbent than the lower concentrations in RH than FRH due to easy access of the mesoporous structure of silica. So with increasing RhB concentrations studied, adsorption capacity of FRH decreases but that of RH increases. This behavior was only observed in RH/FRH adsorbent system because they are two component systems. In single component adsorbents studied, adsorbents of which the surface is not functionalized, CH and SC also behave in the same way that their functionalized counterpart, FCH and FSC. It is important to note that the micropore structure mainly contributes to the adsorption process but the adsorbate molecule should be small enough to reach the micropores. The molecule size of RB is about 1.8 nm and the micropore diameter is less than 2 nm [15]. Therefore, micropore structure is not accessible to RhB molecules and they tend to adsorb to mesopore structure. When the porous structure of RH is considered as it has two components, carbon and silica, micropores are present only in the carbon matrix and mesopores are present in both components. As CH and SC are single component adsorbents the micropores and mesopores of carbon contribute to the adsorption process. But for a constant weight, carbon and silica of RH contributes while only carbon is accountable for the weight of CH and SC. So all together the porous structure naturally available and introduced functional groups contribute to the adsorption process.

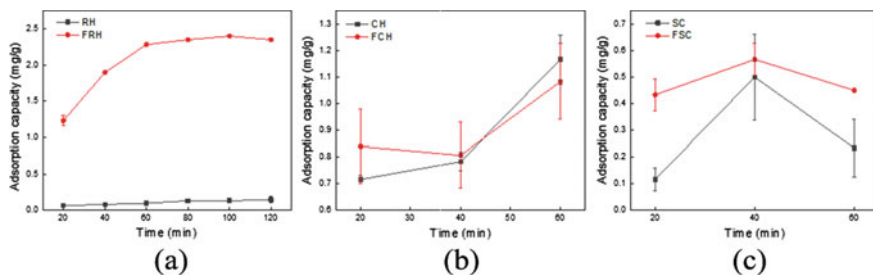


Fig. 6 Effect of initial dye concentration on adsorption of RhB on **a** RH and FRH, **b** CH and FCH, **c** SC and FSC

3.1.7 Effect of Contact Time

RH and FRH were subjected to determine the effect of time on adsorption. As shown in the Fig. 6 adsorption capacity of FRH increases with time up to 60 min followed by constant behavior after that. Behaviour of RH is similar to FRH though the adsorption capacity is very low compared to FRH. As the equilibrium of adsorption has reached in 60 min in FRH and RH, other porous materials were also subjected to the same conditions for one hour. FCH and CH and FSC and SC showed fluctuating adsorption during this time period.

3.1.8 Reusability Study

The reusability of the functionalized adsorbents (FRH, FCH and FSC) were evaluated by using the same amount of functionalized adsorbent for three cycles of adsorption of RhB at the same experimental conditions. Adsorbent was washed with ethanol and distilled water to remove any loosely bound RhB molecules. Figure 7 shows the reusability of the functionalized adsorbents. It could be clearly seen that the adsorption capacity decreases with the number of the cycle used. This could

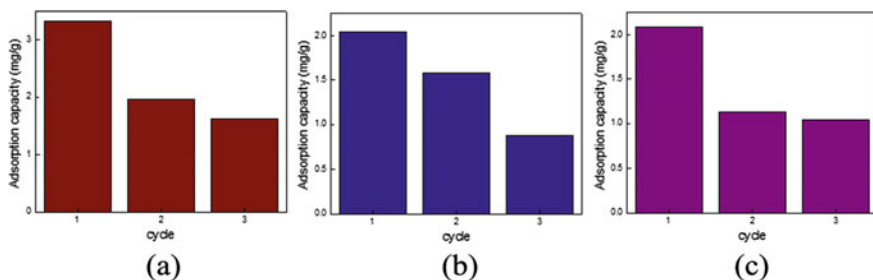


Fig. 7 Reusability of adsorbents on adsorption of RhB on **a** RH and FRH, **b** CH and FCH, **c** SC and FSC

be due to the fact that the adsorption has occur through both chemisorption and physisorption where monolayer of RhB molecules have adsorb to the adsorbent surface through chemisorption and subsequently monolayers of RhB molecules adsorb onto the existing layers via physisorption. Upon washing with distilled water and ethanol physisorbed RhB molcules have washed off. Adsorption capacity has dramatically dropped in the second cycle of all three functionalized adsorbents. This could be because physisorbed RhB molecules remove when the adsorbents are washed with distilled water and ethanol and the chemisorbed molecules are not. So the chemisorbed molecules from the first cycle remains on the adsorbent and on subsequent cycles RhB molecules adsorb only via physisorption. Especially in FRH and FSC the adsorption capacity at the second and third cycles is almost the same with a slight reduction supporting the hypothesis. However, in FCH adsorption capacity keep decreasing.

4 Conclusions

This work compared the adsorption of a dye RhB onto different carbon based adsorbents originated from two different waste materials, rice husk and coconut husk, and porous carbon synthesized by resorcinol formaldehyde polymerization. All the adsorbents were functionalized with nitric acid. Adsorption was determined as a function of pH, amount of adsorbent dose, concentration and contact time. From the results it has been concluded that, all the natural and synthetic adsorbents were effective in removing RhB, while the functionalized adsorbents were much more effective compared to the untreated adsorbents. Functionalized rice husk was much more effective than all other adsorbents and adsorbents derived from natural waste materials were comparatively more effective than the synthetic porous carbon.

Acknowledgements The authors are grateful to Sri Lanka Institute of Nanotechnology for performing the Scanning electron microscopic analysis.

Declaration of Interest The authors declare that they have no competing interests.

References

1. Aboulhassan MA et al (2006) Improvement of paint effluents coagulation using natural and synthetic coagulant aids. *J Hazard Mater* 138(1):40–45. <https://doi.org/10.1016/J.JHAZMAT.2006.05.040>
2. Ahmed MN, Ram RN (1992) Removal of basic dye from waste-water using silica as adsorbent. *Environ Pollut* 77(1):79–86. [https://doi.org/10.1016/0269-7491\(92\)90161-3](https://doi.org/10.1016/0269-7491(92)90161-3)
3. Banerjee S et al (2017) Adsorption characteristics of alumina nanoparticles for the removal of hazardous dye, orange G from aqueous solutions. *Arab J Chem.* <https://doi.org/10.1016/J.ARABJC.2016.12.016>

4. Bharathi KS, Ramesh ST (2013) Removal of dyes using agricultural waste as low-cost adsorbents: a review. *Appl Water Sci* 3(4):773–790. <https://doi.org/10.1007/s13201-013-0117-y>
5. Bhatnagar A, Jain AK (2005) A comparative adsorption study with different industrial wastes as adsorbents for the removal of cationic dyes from water. *J Colloid Interface Sci* 281(1):49–55. <https://doi.org/10.1016/J.JCIS.2004.08.076>
6. Bhattacharyya KG, Sharma A (2004) Azadirachta indica leaf powder as an effective biosorbent for dyes: a case study with aqueous Congo Red solutions. *J Environ Manage* 71(3):217–229. <https://doi.org/10.1016/J.JENVMAN.2004.03.002>
7. Chakrabarti S, Dutta BK (2004) Photocatalytic degradation of model textile dyes in wastewater using ZnO as semiconductor catalyst. *J Hazard Mater* 112(3):269–278. <https://doi.org/10.1016/J.JHAZMAT.2004.05.013>
8. Chen A et al (2016) Synthesis of mesoporous carbon nanospheres for highly efficient adsorption of bulky dye molecules. *J Mater Sci* 51(14):7016–7028. <https://doi.org/10.1007/s10853-016-9991-7>
9. Crundwell FK (2014) The mechanism of dissolution of minerals in acidic and alkaline solutions: Part II application of a new theory to silicates, aluminosilicates and quartz. *Hydrometallurgy* 149:265–275. <https://doi.org/10.1016/J.HYDROMET.2014.07.003>
10. Deshpande AV, Kumar U (2002) Effect of method of preparation on photophysical properties of Rh-B impregnated sol–gel hosts. *J Non-Cryst Solids* 306(2):149–159. [https://doi.org/10.1016/S0022-3093\(02\)01054-2](https://doi.org/10.1016/S0022-3093(02)01054-2)
11. Dotto GL, Pinto LAA (2011) Adsorption of food dyes onto chitosan: optimization process and kinetic. *Carbohydr Polym* 84(1):231–238. <https://doi.org/10.1016/J.CARBPOL.2010.11.028>
12. Garg V et al (2003) Dye removal from aqueous solution by adsorption on treated sawdust. *Biores Technol* 89(2):121–124. [https://doi.org/10.1016/S0960-8524\(03\)00058-0](https://doi.org/10.1016/S0960-8524(03)00058-0)
13. Geçgel Ü, Özcan K, Gürpınar GÇ (2013) Removal of methylene blue from aqueous solution by activated carbon prepared from pea shells (*Pisum sativum*). *J Chem* 2013:1–9. <https://doi.org/10.1155/2013/614083>
14. Gümüş D, Akbal F (2011) Photocatalytic degradation of textile dye and wastewater. *Water Air Soil Pollut* 216(1–4):117–124. <https://doi.org/10.1007/s11270-010-0520-z>
15. Guo Y et al (2005) Use of rice husk-based porous carbon for adsorption of Rhodamine B from aqueous solutions. *Dyes Pigm* 66(2):123–128. <https://doi.org/10.1016/J.DYEPIG.2004.09.014>
16. Gupta VK et al (2010) Equilibrium and thermodynamic studies on the adsorption of the dye tartrazine onto waste “coconut husks” carbon and activated carbon. *J Chem Eng Data* 55(11):5083–5090. <https://doi.org/10.1021/je100649h>
17. Gupta VK et al (2012) Photo-catalytic degradation of toxic dye amaranth on TiO₂/UV in aqueous suspensions. *Mater Sci Eng, C* 32(1):12–17. <https://doi.org/10.1016/J.MSEC.2011.08.018>
18. Han R et al (2010) Characterization of modified wheat straw, kinetic and equilibrium study about copper ion and methylene blue adsorption in batch mode. *Carbohydr Polym* 79(4):1140–1149. <https://doi.org/10.1016/J.CARBPOL.2009.10.054>
19. Hao G-P et al (2011) Structurally designed synthesis of mechanically stable Poly(benzoxazine-co-resol)-based porous carbon monoliths and their application as high-performance CO₂ capture sorbents. *J Am Chem Soc* 133(29):11378–11388. <https://doi.org/10.1021/ja203857g>
20. Hao OJ, Kim H, Chiang P-C (2000) Decolorization of wastewater. *Crit Rev Environ Sci Technol* 30(4):449–505. <https://doi.org/10.1080/10643380091184237>
21. Huang C-H et al (2011) Adsorption of cationic dyes onto mesoporous silica. *Microporous Mesoporous Mater* 141(1–3):102–109. <https://doi.org/10.1016/J.MICROMESO.2010.11.002>
22. Hunger K, Gregory P, Miederer P, Berneth H, Heid C, Mennicke W (2002) Important chemical chromophores of dye classes. *Ind Dye* 13–112. <https://doi.org/10.1002/3527602011.ch2>
23. Kannan N, Sundaram MM (2001) Kinetics and mechanism of removal of methylene blue by adsorption on various carbons—a comparative study. *Dyes Pigm* 51(1):25–40. [https://doi.org/10.1016/S0143-7208\(01\)00056-0](https://doi.org/10.1016/S0143-7208(01)00056-0)

24. Kant R, Kant R (2012) Textile dyeing industry an environmental hazard. *Nat Sci* 04(01):22–26. <https://doi.org/10.4236/ns.2012.41004>
25. Kasperchik VP, Yaskevich AL, Bil'dyukevich AV (2012) Wastewater treatment for removal of dyes by coagulation and membrane processes. *Pet Chem* 52:545–556. <https://doi.org/10.1134/S0965544112070079>
26. Khodaie M et al (2013) Removal of methylene blue from wastewater by adsorption onto ZnCl₂ activated corn husk carbon equilibrium studies. *J Chem* 2013:1–6. <https://doi.org/10.1155/2013/383985>
27. Liang C, Dai S (2009) Dual phase separation for synthesis of bimodal meso-/macroporous carbon monoliths. *Chem Mater* 21(10):2115–2124. <https://doi.org/10.1021/cm900344h>
28. Malik PK (2004) Dye removal from wastewater using activated carbon developed from sawdust: adsorption equilibrium and kinetics. *J Hazard Mater* 113(1–3):81–88. <https://doi.org/10.1016/J.JHAZMAT.2004.05.022>
29. Mane VS, Deo Mall I, Chandra Srivastava V (2007) Kinetic and equilibrium isotherm studies for the adsorptive removal of Brilliant Green dye from aqueous solution by rice husk ash. *J Environ Manage* 84(4):390–400. <https://doi.org/10.1016/J.JENVMAN.2006.06.024>
30. Mohammadi M et al (2010) Removal of Rhodamine B from aqueous solution using palm shell-based activated carbon: adsorption and kinetic studies. *J Chem Eng Data* 55(12):5777–5785. <https://doi.org/10.1021/je100730a>
31. Namasivayam C, Kavitha D (2002) Removal of congo red from water by adsorption onto activated carbon prepared from coir pith, an agricultural solid waste. *Dyes Pigm* 54(1):47–58. [https://doi.org/10.1016/S0143-7208\(02\)00025-6](https://doi.org/10.1016/S0143-7208(02)00025-6)
32. Popli S, Patel UD (2015) Destruction of azo dyes by anaerobic–aerobic sequential biological treatment: a review. *Int J Environ Sci Technol* 12(1):405–420. <https://doi.org/10.1007/s13762-014-0499-x>
33. Raghuvanshi S, Singh R, Kaushik CP, Raghav A (2004) Kinetics study of methylene blue dye bioadsorption on baggase, Epa.Niif.Hu. (n.d.). http://epa.niif.hu/02500/02583/00003/pdf/EPA_02583_applied_ecology_2004_02_035-043.pdf (accessed October 6, 2019)
34. Ramuthai S et al (2009) Rhodamine B adsorption-kinetic, mechanistic and thermodynamic studies. *E-J Chem* 6(s1):S363–S373. <https://doi.org/10.1155/2009/470704>
35. Rangabhashiyam S et al (2015) Biosorption potential of a novel powder, prepared from *Ficus auriculata* leaves, for sequestration of hexavalent chromium from aqueous solutions. *Res Chem Intermed* 41(11):8405–8424. <https://doi.org/10.1007/s11164-014-1900-6>
36. Shokri B, Firouzjah MA, Hosseini SI (2009) FTIR analysis of silicon dioxide thin film deposited by metal organic-based PECVD. In: *Proceeding 19th International Plasma Chemical Society* 1–4. <https://www.ispc-conference.org/>
37. Sivaraj R, Namasivayam C, Kadirvelu K (2001) Orange peel as an adsorbent in the removal of Acid violet 17 (acid dye) from aqueous solutions. *Waste Manage* 21(1):105–110. [https://doi.org/10.1016/S0956-053X\(00\)00076-3](https://doi.org/10.1016/S0956-053X(00)00076-3)
38. Smith B (2018) Infrared spectral interpretation: a systematic approach. <https://content.taylorfrancis.com/books/download?dac=C2006-0-03642-5isbn=9780203750841format=googlePreviewPdf> (accessed October 15, 2019)
39. Sumathi S et al (2010) Selection of best impregnated palm shell activated carbon (PSAC) for simultaneous removal of SO₂ and NO_x. *J Hazard Mater* 176(1–3):1093–1096. <https://doi.org/10.1016/J.JHAZMAT.2009.11.037>
40. Thakur A, Kaur H (2017) Response surface optimization of Rhodamine B dye removal using paper industry waste as adsorbent. *Int J Ind Chem* 8(2):175–186. <https://doi.org/10.1007/s40090-017-0113-4>
41. Thambiliyagodage CJ, Cooray VY, Perera IN, Wijesekera RD (2020) Eco-friendly porous carbon materials for wastewater treatment. In: Springer, Singapore, pp. 252–260. https://doi.org/10.1007/978-981-13-9749-3_23
42. Vlyssides A et al (2000) Testing an electrochemical method for treatment of textile dye wastewater. *Waste Manage* 20(7):569–574. [https://doi.org/10.1016/S0956-053X\(00\)00028-3](https://doi.org/10.1016/S0956-053X(00)00028-3)

43. Wang S, Li H, Xu L (2006) Application of zeolite MCM-22 for basic dye removal from wastewater. *J Colloid Interface Sci* 295(1):71–78. <https://doi.org/10.1016/J.JCIS.2005.08.006>
44. Yagub MT et al (2014) Dye and its removal from aqueous solution by adsorption: a review. *Adv Coll Interface Sci* 209:172–184. <https://doi.org/10.1016/J.CIS.2014.04.002>
45. Yu J-X et al (2009) Polymer modified biomass of baker's yeast for enhancement adsorption of methylene blue, rhodamine B and basic magenta. *J Hazard Mater* 168(2–3):1147–1154. <https://doi.org/10.1016/J.JHAZMAT.2009.02.144>
46. Zhang G et al (2008) The surface analytical characterization of carbon fibers functionalized by H₂SO₄/HNO₃ treatment. *Carbon* 46(2):196–205. <https://doi.org/10.1016/J.CARBON.2007.11.002>